Journal of Radiotherapy in Practice

Journal of Radiotherapy in Practice 2003
3, 123–129
© Greenwich Medical Media Ltd. 2003

Original Article

Absolute radiation dose verification using magnetic resonance imaging: feasibility study

G. P. Liney, A. Heathcote†, A. Jenner†, L. W. Turnbull, A. W. Beavis‡

Centre for MR Investigations, Hull Royal Infirmary; †Department of Physical Sciences, University of Hull; ‡Department of Radiation Physics, Princess Royal Hospital, Hull, UK

Abstract

This work describes the feasibility of using a polymer-based tissue equivalent gel for measuring radiation doses in situ. The gel is based on the MAGIC formulation thereby enabling it to be manufactured under normal atmospheric conditions. Its composition has been altered to achieve a similar sensitivity to the more widely used, but technically more difficult to produce, PAG gels. Irradiation of the gel material causes polymerisation of the molecular structure resulting in a shortening of transverse relaxation time (T_2), which can be imaged using Magnetic Resonance Imaging (MRI). This work calibrates the radiation response in terms of transverse relaxation rate (R_2) and uses this information to provide absolute dose verification in a separate gel, which has been previously irradiated to a known configuration. Results demonstrate that this technique is able to verify radiation doses to within a few percent of delivered intent in three dimensions and with high spatial resolution. This work may be followed by anyone with an interest in the quality assurance of advanced conformal radiotherapy delivery methods.

Keywords

IMRT; gel dosimetry; MRI

INTRODUCTION

In conformal therapy an increase in the therapeutic ratio is sought; this can be achieved by an increase in control of the disease or by a reduction in the adverse affects to proximal normal tissues. The radiotherapy community is witnessing a revolution in radiotherapy technology whereby commercial planning and delivery solutions are enabling advanced conformal techniques such as Intensity Modulated Radiotherapy (IMRT)[1] to become more widely utilised. However, these advanced approaches to treatment delivery, with beams that dynamically change during their delivery, have rendered traditional quality control solutions inadequate. Currently, dose verification and quality assurance of IMRT is typically performed using appropriate X-ray film. This methodology is not ideal, due to its inherent two-dimensional limitations. Furthermore, the film has a much higher density than tissue and so very careful calibration techniques are required to gain accurate results.[2] Three-dimensional distributions can be measured by using phantoms incorporating a stack of films positioned at various planes, thereby recording

Correspondence to: Dr Gary P. Liney, Centre for MR Investigations, Hull Royal Infirmary, Hull, HU3 2JZ, UK. E-mail: g.p.liney@hull.ac.uk
This work has been funded by a grant from Yorkshire Cancer Research.

https://doi.org/10.1017/S1460396903000128 Published online by Cambridge University Press

doses with improved coverage. A true three-dimensional solution requires the ability to make measurements at much greater through-plane spatial resolution without the need to specifically construct test objects.

The use of tissue-equivalent gels to provide these dose measurements has been of interest to various research groups over the last few years. The gels are irradiated and subsequently characterised using some three-dimensional imaging modality, which in the vast majority of cases, has been Magnetic Resonance Imaging (MRI). Initially much work focused on so-called Fricke gels, which were comprised of an aqueous gel infused with Fricke ferrous sulphate solution.[3] The gel worked by producing free radicals from the radiolysis of water, which oxidised ferrous ions into ferric ions. The change in magnetic susceptibility caused by this process enabled the dose distributions to be demonstrated on MRI and these could be calibrated from the resulting change in T_1 relaxation time. Unfortunately these gels suffered from ferric ion diffusion following irradiation, which effectively blurred the dose distributions and limited their usefulness. This is especially important in modern IMRT delivery, where high spatial gradients can exist "everywhere"! Solutions to this problem have been to either reduce the diffusion mechanism by using PVA-based formulations[4] or acquiring much faster MRI measurements using calibrations based on relative signal changes rather than absolute T_1 measurements.[5]

In 1994 Maryanski et al.[6] introduced a new generation of polymer gels composed of acrylamide set in gelatin (referred to here and in the literature as PAG). These gels contain acrylic monomer units, which polymerise during irradiation and can be interrogated with MRI due to the resulting relaxation time shortening. These gels have several advantages over Fricke gels. Firstly, they are inherently more stable and can be used to produce calibration curves, which demonstrate little change in the slope or intercept over time.[7] Secondly, the gels are more sensitive to radiation than Fricke gels. Thirdly, the radiation-induced polymers are insoluble and the altered optical density of the gel permits a visual inspection of the irradiation and opens up the possibility of using a cheaper optical based scanning technique.[8] However, much of the work to date has investigated their use in conjunction with MRI. In MRI, both T_1 and T_2 relaxation times are affected, causing hyper- and hypointensity in the irradiated region respectively, although the latter effect is more pronounced. The radiation changes can be demonstrated with both MR imaging and spectroscopy[9] though our own experience has found that the dynamic range of the spectroscopy changes to be disappointing, with only a 10% difference in spectral profile between 0 and 10 Gy.[10]

The use of PAG gels is not without their own difficulties. Commonly used ingredients such as bis and acrylamide (BANG™ gels) need careful handling, as the constituents are neurotoxins and carcinogens. Manufacturing and storage has to be in a strictly oxygen-free environment. This is to prevent the oxygen inhibition of the polymerisation process and has ultimately led to their limited clinical application as dosimeters. In order to simplify the production and reduce the sensitivity to oxygen new generations of polymer gels have been devised. Fong et al.[11] introduced the first "normoxic" gel in which a bivalent metal (copper) complexes with ascorbic acid in the presence of oxygen to generate free radicals which then initiates the polymerisation process. In this case oxygen is required and the gels can be made and used without the earlier restrictions. This gel is known as MAGIC (Methacrylic acid, Ascorbic acid, Gelatin Instigated by Copper) and is the basis of the work described here. Fong et al. showed that by altering the concentrations of methacrylic acid some alteration in the calibration characteristics could be observed.

This study has adapted Fong's work and produced a simple gel-dosimeter with improved sensitivity and extended linearity compared to PAG gels. A calibration has been obtained and this has been used to verify doses in a separate flask, which had been previously irradiated with a parallel pair of opposing beams. Results demonstrate the accuracy of the technique and the feasibility of using MRI for providing dose mapping at high spatial resolution. The intention of this paper is to illustrate the ease with which gel dosimetry may be performed and to stimulate interest in this field.

https://doi.org/10.1017/S1460396903000128 Published online by Cambridge University Press

METHODS

The MAGIC gel was prepared using the following ingredients: gelatin (300 bloom), 80 grams per litre (~8% by weight); hydroquinone, 1.8×10^{-2} M; ascorbic acid, 2.0×10^{-3} M; copper (II) sulphate pentahydrate 99.9%, 8.0×10^{-5} M; methacrylic acid 99%. The manufacture of 1 litre of the gel (at a strength of methacrylic acid (MAA) of 9%) can be summarised as follows. Firstly, 700 ml of water is heated to 50°C and the gelatin added. Two grams of hydroquinone in 48 ml of distilled water is added at this stage and the mixture is allowed to cool. At 37°C, 0.352 g of ascorbic acid in 50 ml of water and 0.020 g of copper sulphate in 30 ml of water is added. Finally 90 g of methacrylic acid is added and the mixture is transferred to suitable containers, which are then sealed and permitted to cool to room temperature and set into a translucent gel. While the quality of the glassware used is not important from the MR imaging point of view, we have chosen to use bottles from a specialised glass-blower rather than mass produced containers which are produced in two halves and as a result are of poor quality with vertical defects. This becomes a crucial consideration if an optical scanning technique is to be used, as is the case in a study we are running in parallel to this work. We have investigated various concentrations of MAA from 3 to 12% in an attempt to reproduce the sensitivity of PAG gels.

It is crucial that both the calibration and verification stages use gel from the same batch. For the calibration step the gel is poured into several 125 ml bottles (Wheaton Science Products, NJ, USA) with diameter × height of 48 × 112 mm. One of these is the control and is left unirradiated, while the remaining bottles were irradiated uniformly, using a parallel pair, to receive incremental doses from (typically) 4 to 30 Gy. The radiation was delivered using 6 MV X-ray beams from a Varian 600C Series Linear Accelerator. A separate large 500 ml glass flask ("test distribution flask" with diameter × height of 91 × 95 mm) filled with gel from the identical batch was irradiated using a parallel pair of 3 cm wide opposing beams to obtain a uniform dose of 5 Gy in the flask. The flask was then rotated through 90° and a second dose of 10 Gy was given. The combined effect produced a "crossfire" of irradiated gel such that the center of the cross received 15 Gy.

All MR imaging was performed on a 1.5 Tesla GE Signa scanner using a commercial radio-frequency head coil. Following initial sagittal localiser images, a T_2-mapping protocol was acquired as described in our previous work.[12] The sequence used was a dual-echo fast spin-echo (FSE) pulse sequence with four echoes acquired over two acquisitions (TE/TR = 30,105 and 60,180 ms/4 s). In the case of the 12% MAA mixture this protocol was altered to make use of shorter echo times with TE values of 20, 30, 70 and 90 ms. This was to account for the increased attenuation at the longer echo times and at doses greater than 20 Gy. In all cases a field-of-view of 24 cm was used with an image matrix of 256 × 256, giving an in-plane resolution of 0.9 mm. Images were obtained throughout the entire volume of the calibration vessels and the test distribution flask acquired in the coronal plane, with a slice thickness of 5 mm and an interslice gap of 1.5 mm. The total scan time of each FSE sequence was approximately 3 minutes, giving a total examination time for calibration and verification of 15 minutes.

Regions-of-interest (ROI) were defined in each of the calibration vessels at each slice location using Advantage Windows software (GE Medical Systems). Mean values of signal intensity were recorded at each echo time and the logarithm of the signal intensity determined. These values were fitted to the following equation using linear regression.

$$\ln S(TE) = \ln S_0 - R_2(D) \cdot TE \qquad [1]$$

where S(TE) is the measured MR signal intensity at a given echo time, TE, S_0 the signal at TE = 0, and $R_2(D)$ is the transverse relaxation rate, being a function of dose. A calibration was established by plotting the estimated R_2 for each known dose value.

Images of the test distribution flask were then transferred to a Sun Workstation whereby in-house software was utilised to re-arrange the order of the image data and produce absolute dose maps. Pixel intensity values were used in the manner described above to determine R_2. These values were then

https://doi.org/10.1017/S1460396903000128 Published online by Cambridge University Press

used to infer dose, D, from the above calibration data as follows:

$$R_2(D) = R_2^0 + \frac{\Delta R_2}{\Delta D} \cdot D \qquad [2]$$

where R_2^0 is the intercept and $\Delta R_2/\Delta D$ is the slope of the fitted line to the calibration data respectively. As an indication of the sensitivity of each gel as a dosimeter the ratio of the slope of the fitted line to the intercept value was made.[11]

After a period of three weeks a calibration was once again established in order to examine the stability of the gel. This was used to re-calculate the dose distributions in the test flask.

RESULTS

Figure 1 illustrates the typical results obtained from the calibration of the dose response. Figure 1(a) shows a T_2-weighted coronal image of the calibration vessels demonstrating the increased signal attenuation, which is observed with incremental dose. Figure 1(b) gives example calibration plots of transverse relaxation rate (R_2) against known radiation dose for three batches of the MAGIC type gel dosimeter made with different concentrations of MAA. For comparison, our previously obtained data using a PAG-type gel[12] is also displayed on the same plot. In contrast to the PAG gel, which only demonstrates a linear dose-R_2 relationship below 10 Gy, the MAGIC gels have an effective range of up to 30 Gy. When linear regression was performed on each of the data (excluding the 10 Gy value for PAG) this gave $R^2 = 0.98$, 0.99 and 0.99 for the MAGIC gels and $R^2 = 0.97$ for the PAG gel. The equations of best fit gave the following values for slope and intercept; 0.26 and 4.08 (3% MAA); 0.56 and 1.91 (9% MAA); 1.19 and 5.25 (12% MAA); 0.32 and 1.25 (PAG).

The plot also demonstrates the degree to which the dose response of the gel can be altered by varying the concentration of methacrylic acid. The ratio of the slope to intercept of each line was 0.06, 0.29 and 0.23 for the MAGIC gels using concentrations of 3.0%, 9.0% and 12% respectively. The corresponding value for the PAG gel sample was 0.26.

Figure 2 demonstrates T_2-weighted coronal images acquired in the large test flask. The images correspond to echo times of (a) TE = 30 ms,

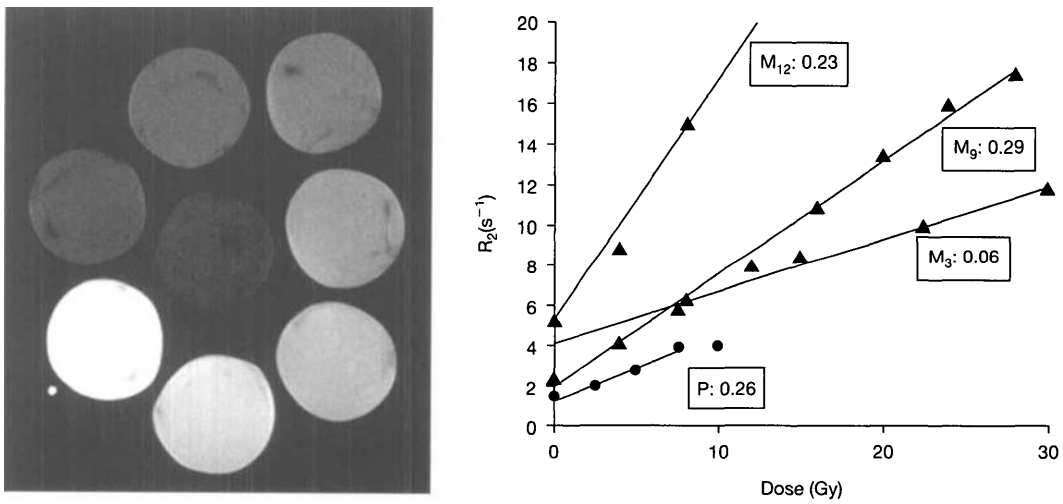


Figure 1. (a) A T_2-weighted image (TE = 105 ms) of the calibration vessels. The control flask is left unirradiated (indicated by a marker) and the rest have received incremental doses in steps of 4 Gy (anticlockwise and inwards). (b) Calibration plot of delivered radiation dose (Gy) against transverse relaxation rate (R_2) for different types of gel dosimeter. Results illustrate the difference in the linearity range of PAG gels (P; circles) compared to the MAGIC gels (M_3, M_9, and M_{12}; triangles corresponding to 3%, 9% and 12% MAA (first three points only shown) respectively). The figure alongside each plot is the ratio of the slope to the intercept, which is an indication of sensitivity; the highest sensitivity of MAGIC gel was achieved using 9% concentration of MAA.

https://doi.org/10.1017/S1460396903000128 Published online by Cambridge University Press

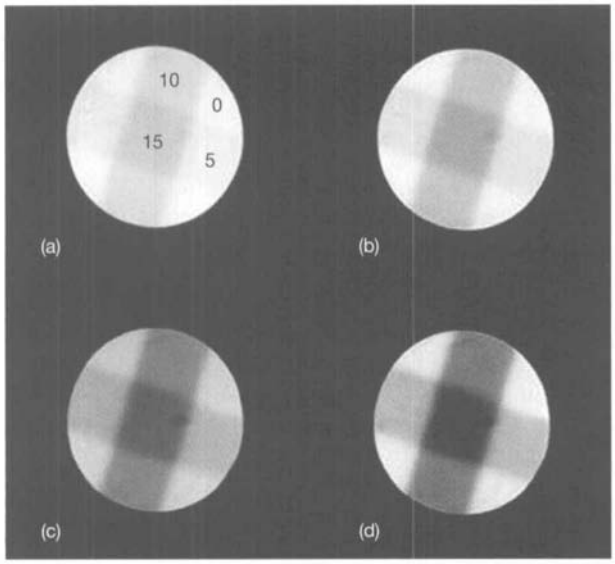


Figure 2. T_2-weighted images (TE = 105 ms) acquired in a MAGIC gel sample which has been irradiated with two 5 Gy and 10 Gy beams to produce a cross configuration giving an isodose of 15 Gy at the centre of the sample. The images are acquired with increasing echo times (TE = (a) 30 ms, (b) 60 ms, (c) 105 ms and (d) 180 ms) and demonstrate increased signal attenuation with increasing dose. These separate echo images enable the transverse relaxation rate to be measured on a pixel-by-pixel basis ($R_2 = 1/T_2$).

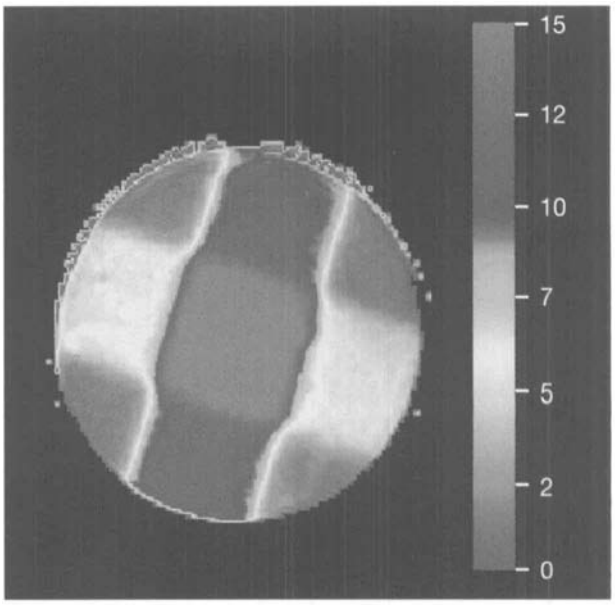


Figure 3. A calculated dose map from the data in Figure 2. By fitting to the signal decay shown in Figure 2 and obtaining a map of R_2, the calibration data can be used to infer a map of absolute radiation dose.

(b) 60 ms, (c) 105 ms and (d) 180 ms respectively. The actual dose values of each region are shown in Figure 2(a). At the longer echo times, the relative doses can be discriminated (in the grey scales) due to the increased signal attenuation caused by the relaxation shortening effects of radiation-induced polymerisation. The signal-to-noise in all images was excellent, and even in the worst case (longest echo time, highest dose) it was three times that of the background signal enabling a good fit to the pixel data.

In Figure 3 the actual dose map is demonstrated using a colour scale with a minimum and maximum set at 0 and 15 Gy. This was calculated by fitting pixel intensity values to equation [1] and using the predicted R_2 values to infer the dose from equation [2]. The calibration in this particular batch (9% MAA) revealed a value for the gradient and intercept of 0.51 and 2.06 respectively. Regions of interest were drawn in each of the areas corresponding to actual doses of 0, 5, 10 and 15 Gy and the corresponding calculated values were 0.7, 4.7, 9.1 and 15.4 Gy respectively. Figure 4 plots the

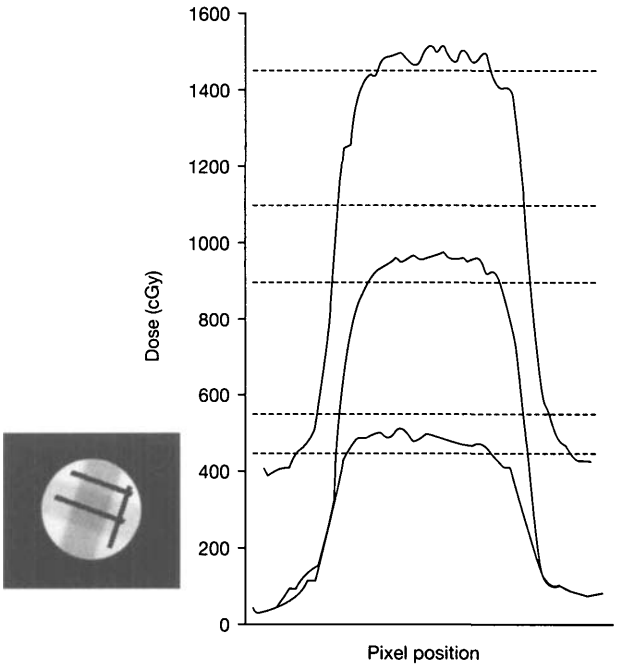


Figure 4. A plot of dose profiles taken across the image in Figure 3 (indicated by insert) illustrating dose changes from 0–5 Gy, 0–10 Gy and 5–15 Gy. The dashed line indicates values within ± 10% of each isodose.

https://doi.org/10.1017/S1460396903000128 Published online by Cambridge University Press

dose profiles taken from regions of interest drawn in the map in Figure 3 across the 0 to 5 Gy, 0 to 10 Gy and 5 to 15 Gy boundaries respectively. The resolution of the dose edges (taken as the FWHM of the differentiation of the profile) is approximately 4.5 pixels (~4 mm) in each case. After three weeks the calibration and verification flasks were re-scanned. The characteristics of the gel had changed considerably (slope and intercept equal to 1.04 and 7.3) and resulted in a decrease in verification accuracy; the agreement was only accurate to 20%.

DISCUSSION

This study has demonstrated the efficacy of using MRI gel dosimetry to accurately verify delivered intent. A technique, which is able to accurately verify radiation doses and demonstrate high dose gradients over a small distance is essential if the full potential of advanced conformal treatments is to be realised. Much of the work in this area to date has used PAG gels to demonstrate dose distributions. Promising results have been obtained, although the majority of studies have only been able to show relative dose measurements with any degree of accuracy and have overestimated absolute values by between 18 and 24%.[9,14] In our own studies we have been able to demonstrate quite a wide range of accuracy with PAG gels (typically between 2 and 30%) and ultimately decided to pursue other dosimeters due to their inherent difficulty in manufacture and the resulting poor reproducibility. Results shown here with MAGIC gels have improved on the sensitivity of PAG gels and also offer the advantage of the simplified manufacturing process and ease of use. These results, examining three dose regions, suggest an accuracy of at least 9%. Furthermore the MAGIC gels provide an extended useful dose range compared to PAG gels. The stability of MAGIC gels also appears to be good with an optimum imaging time of 30 hours following irradiation being reported in one study.[15] We have shown that considerable changes occur in the MAGIC gel after three weeks, which reduced the verification accuracy even when a new calibration was acquired at this time.

Crucial to the success of this technique is the accuracy of the T_2 mapping sequence used as the basis of both the calibration and the verification. A study of some of the various MRI sequences has been examined comparing the accuracy over a range of T_2 values between 140–700 ms.[16] This study assumed the dosimeter was PAG-based, but the T_2 values corresponding to MAGIC gels are somewhat smaller (see Fig. 1). The reliability of the T_2 measurements will depend on the choice of pulse sequence and the range of echo times used to sample the signal decay. In this work we had to modify our echo times for the 12% MAA gel in order to accommodate the rapid signal attenuation observed at high dose levels. We have previously demonstrated the accuracy of our FSE sequence in a clinical situation although it is important to ascertain the best sequence on each particular system. Assuming an expected T_2 measurement accuracy of 10% and considering a gel sensitivity of 0.29 (M_9 in Fig. 1b), a dose resolution of approximately 0.5 Gy should be possible. Certainly, the FSE sequence provides inherently fast T_2-weighted images and can be used efficiently over a large volume coverage. For example, in our protocol up to 22 slices can be acquired in less than 6 minutes, which may be reduced to three minutes if a two-point calculation is required.

An important consideration in this work is the attainable spatial resolution. In this study an in-plane resolution of 0.9 mm was used in both the calibration and verification process. This has provided adequate signal-to-noise even for TE = 180 ms and the highest dose values. By using a true 3D image acquisition (compared to multi-slice 2D imaging) a more isotropic resolution (typically 1 mm in each direction) could be realised albeit with a slight increased time penalty.

While the gels in their current formulation seem to provide excellent accuracy and reproducibility there is a great deal of potential for exploiting the Chemistry still further. For example the increased concentration of MAA has increased the slope of the calibration curve but at 12% MAA this has also lead to an increased background polymerisation, increasing the value of the intercept and therefore having a detrimental effect on sensitivity. This would therefore imply that there is an optimal value of MAA concentration, between 9% and 12%, in which the sensitivity is maximised. In addition there may be more suitable anti-oxidants

https://doi.org/10.1017/S1460396903000128 Published online by Cambridge University Press

to use rather than copper, which will further simplify the preparation and usefulness of these gels.[17] The rate of cooling needs further attention to minimise the inhomogeneities in the mixture that arise near the top of the containers. These can be seen in Figure 1 as irregular hypointense streaks in the gel and will result in tiny areas of artificially high dose in the final map. We are presently investigating the use of ice-cooling as a method of preventing these artifacts.

In our on-going work we are developing a complete quality assurance test object, including anatomically related compartments and markers for measuring image distortion.[18] It will also incorporate a removable gel flask for dose verification in the manner described above. In the future the current trend to move towards higher magnetic field strength will see further improvements in image signal-to-noise and therefore spatial resolution. This seems certain to extend the role of MRI in radiotherapy practice from treatment planning to dose verification.

Acknowledgements

The authors would like to express their gratitude to Yorkshire Cancer Research for providing a grant to fund this work.

References

1. Webb S. Intensity Modulated Radiation Therapy. Bristol: IOP Publishing, 2000.
2. Beavis AW, Weston SJ, Whitton VJ. Implementation of the Varian EDW into a commercial RTP system. Phys Med Biol 1996; 41(9): 1691–1704.
3. Gore JC, Kang YS, Schulz RJ. Measurement of radiation distribution by nuclear magnetic resonance (NMR) imaging. Phys Med Biol 1984; 29: 1189–1197.
4. Chu KC, Jordan KJ, Battista JJ, Van Dyk J, Rutt BK. Polyvinyl alcohol-Fricke hydrogel; and cryogel: two new gel dosimetry systems with low Fe3+ diffusion. Phys Med Biol 2000; 45: 955–969.
5. Chu WC, Guo WY, Wu MC, Chung WY, Pan DHC. The radiation induced magnetic resonance imaging intensity change provides a more efficient three-dimensional dose measurement in MRI-Fricke-agarose gel dosimetry. Med Phys 1998; 25: 2326–2332.
6. Maryanski MJ, Schulz RJ, Ibbott GS, et al. Magnetic resonance imaging of radiation dose distributions using a polymer-gel dosimeter. Phys Med Biol 1994; 39: 1437–1455.
7. Cosgrove VP, Murphy PS, McJury PS et al. The reproducibility of polyacrylamide gel dosimetry applied to stereotactic conformal radiotherapy. Phys Med Biol 2000; 45: 1195–1210.
8. Gore JC, Ranade M, Maryanski MJ, Schulz RJ. Radiation dose distributions in three dimensions from tomographic optical density scanning of polymer gels: I. Development of an optical scanner. Phys Med Biol 1996; 41: 2695–2704.
9. Murphy PS, Cosgrove VP, Schwarz AJ, Webb S, Leach MO. Proton spectroscopic imaging of polyacrylamide gel dosimeters for absolute radiation dosimetry, Phys Med Biol 2000; 45: 835–845.
10. Liney GP, Manton DJ, Hutton J, Beavis A, Turnbull LW. MRI and MRS of radiation distributions using a polymer-gel dosimeter. Proceedings 9th Meeting of the International Society for Magnetic Resonance in Medicine 2001; 903.
11. Fong PW, Keil DC, Dose MD, Gore JC. Development of "normoxic" polymer gels for MRI dosimetry. Proceedings of DOSGEL, 2001.
12. Liney GP, Knowles AJ, Manton DJ, Turnbull LW, Blackband SJ, Horsman. Comparison of conventional single echo and multi-echo sequences with a fast spin-echo sequence for quantitative T_2 mapping: application to the prostate. J Magn Reson Imag 1996; 6: 603–607.
13. Liney GP, Beavis AW, Goodby JW, Turnbull LW. Calibrating radiotherapy doses using MRI. Magnetic Resonance Materials in Phys Biol Med 2002; 15(S1): 480.
14. Meeks SL, Bova FJ, Maryanski MJ. Image registration of BANG gel dose maps for quantitative dosimetry verification. Int J Radiat Oncol 1999; 43: 1135–1141.
15. De Deene Y, Venning A, Hurley C, Healy BJ, Baldock C. Dose-response stability and integrity of the dose distribution of various polymer gel dosimeters. Phys Med Biol 2002; 47: 2459–2470.
16. Baustert IC, Oldham M, Smith TAD, Hayes C, Webb S, Leach MO. Optimised MR imaging for polyacrylamide gel dosimetry. Phys Med Biol 2000; 45: 847–858.
17. De Deene Y, Hurley C, Venning A, et al. A basic study of some normoxic polymer gel dosimeters. Phys Med Biol 2002; 47: 3441–3463.
18. Moore CS, Liney GP, Beavis AW. Quality assurance of CT and MR registration for radiotherapy planning of head and neck cancers. Clin Oncol 2003; 15: S8.

https://doi.org/10.1017/S1460396903000128 Published online by Cambridge University Press